AAS 24-279

CONCEPTUAL SPACES FOR COLLISION RISK ASSESSMENT

Benjamin L. Reifler,[*] S. Anand Agrawal,[*] Mitchell D. Rosen,[†] Kanak Parmar,[‡] Brandon A. Jones,[§] Nathan Ré[¶]

This work proposes a framework for collision risk assessment based on the theory of conceptual spaces. Conceptual spaces define human concepts with geometry and may be used as a means of hard and soft information fusion. The approach in this paper leverages orbital mechanics to determine one satellite's ability to reach another in a given timeframe and soft information to determine whether or not this reachability constitutes a real risk. The conceptual spaces-based risk analysis produces an earlier warning than a traditional collision probability analysis when applied to a historical collision scenario.

INTRODUCTION

The space environment around Earth is expected to become increasingly congested over the next few decades as interest in developing and launching satellite constellations grows. With 58,000 additional satellites expected in Earth orbit by 2030,[1] collision avoidance systems will be paramount to protecting these assets and mitigating their contributions to orbital debris growth. Determining collision probability between two objects is key to current collision avoidance strategies.[2] Collision probability calculations rely on observable hard data including both spacecrafts' nominal orbits and position errors, often with Gaussian assumptions for the underlying distributions.[3] However, other criteria such as mission criticality and maneuver capability may justify earlier action than suggested by probability of collision. These criteria are examples of soft data, which are contextualized by human perception, and are difficult to capture in traditional analysis frameworks. Conceptual spaces offer a means to further inform collision risk through hard and soft information fusion.

The theory of conceptual spaces translates human concepts into geometry.[4] In this paper, we present a conceptual space to characterize collision risk. Hard and soft information are combined to determine one satellite's ability to reach another in a given timeframe and whether or not this reachability constitutes actionable risk. Our scheme can account for uncertainty in orbit determination (OD) and the observed soft information. We apply our conceptual spaces-based risk analysis to a real collision scenario and find that it produces an earlier warning than a traditional collision probability analysis based on historical tracking data leading up to that collision.

Human ideas including risks, beauty, and value can be defined through the conceptual space paradigm. There are four building blocks to a conceptual space: dimensions, domains, properties,

[*]Graduate Research Assistant, The University of Texas at Austin, Student Member AIAA.
[†]Staff Astrodynamics and Satellite Navigation Engineer, Advanced Space, LLC.
[‡]Staff Astrodynamics and Satellite Navigation Engineer and Machine Learning Specialist, Advanced Space, LLC.
[§]Associate Professor, The University of Texas at Austin, Associate Fellow AIAA.
[¶]Principal Astrodynamics, Satellite Navigation, and Machine Learning Engineer, Advanced Space, LLC.

and concepts.[4] Dimensions represent the unique quality attributes of a conceptual space.[5] Domains are sets of dimensions that are related to one another in such a way that it is logical to consider all of them when defining the distance between two points in that domain. For instance, hue, saturation, and brightness could be dimensions in a color domain.[4] Dimensional representations of domains are often difficult to identify, and instead domains and properties can be used.[6] Properties materialize the dimensions into tangible ideas, and are considered combinations of dimensions within a single domain. Geometrically, properties are convex regions of domains. Concepts can be thought of as manifestations of specific properties from each domain and combinations of properties from several domains (cross-domain associations). Conceptual space paradigms are useful when trying to map observations to concepts; this process is commonly framed with optimization. Each concept corresponds to a set of constraints and an objective function, which are used to calculate the similarity between a set of observations and the concept.

The fusion of hard and soft data in conceptual spaces manifests in several ways. Conceptual space dimensions are often defined with hard information. For example, the brightness dimension in the color domain discussed above can be quantified with luminance or apparent magnitude. Similarity values, which represent an observable parameter or measurement, frequently enter the conceptual space optimization problem as hard data. The soft information can also be transcribed into quantitative constraints, see Table 1. Such information fusion via conceptual spaces has been previously explored in space situational awareness (SSA) applications for threat assessment.[7–9] In contrast, we utilize domain and property relationships and not explicit dimensions to define concepts, have a simplified ontology that ignores operator intent, and introduce a novel method for handling uncertainty in the observations. This paper's contributions to the SSA literature are a new operator-focused conceptual spaces paradigm for collision risk, a novel interpolation method to include uncertainty in reachability measurements, and a case study using a historical space collision (the 2009 collision between Iridium 33 and Cosmos 2251).

METHODOLOGY

Overview

Our conceptual space scheme leverages domain and property relationships to determine whether a satellite poses a collision risk to another satellite. This conceptual space utilizes multiple domains, each with multiple properties, to define concepts. This is called a *complex conceptual space*.[4] The conceptual space and concept definitions presented here are an initial attempt and informed by our thinking of what spacecraft operators may find relevant. The domains and properties of our risk conceptual space are:

1. Propulsion: Chemical, Electrical, None;
2. Maneuverability: Healthy, Defunct;
3. Reachability: Short, Medium, Long, Never;
4. Vulnerability: Yes, No.

Dimensions are not explicitly defined. The reachability properties reflect the time it would take for the chaser to collide with the object under consideration based on its assumed available Δv. Due to uncertainty in OD and in the available Δv, the reachability observations include uncertainty that must be considered.

Reachability is assessed in the short, medium, and long terms to contextualize risk of collision both immediately and in the near future. The reachability study has separate tools for high and low thrust propulsion systems. Each tool presently assumes a two-body dynamics model with the Earth J_2 effect applied. The high thrust reachability software determines the minimum Δv required for the chaser to impact a given object. The tool considers collision trajectories with up to two maneuvers. The low thrust configuration generates a multi-dimensional space of orbital elements that can be reached by the chaser within a set time period; spacecraft within this space are considered to be collision risks. The low thrust tool's reachable space is created by feeding randomly sampled initial costates into a solver that propagates the states for some duration within the set time period. Both the high and low thrust tools generate inputs for the conceptual spaces model that characterize possible impacts.

To calculate how similar a set of observations $\boldsymbol{s}$ is to a given concept c, we determine the set of properties that an instance of c could have—given the definition of c—that maximizes the sum of observed similarity values s_{ij} for each included property x_{ij}.[4] This is equivalent to the following mixed integer optimization problem:

$$\max_{\boldsymbol{x}} f_c(\boldsymbol{x} \mid \boldsymbol{s}) \quad \text{subject to} \quad g(\boldsymbol{x}) \leq 0 \wedge h(\boldsymbol{x}) = 0\,, \tag{1}$$

where $\boldsymbol{x} = [x_{11} \;\; x_{12} \;\; \ldots]^\mathsf{T}$ is a vector of binary states that determine which properties are active, f_c is the weighted average of observed similarity values for each active property, and g and h are a set of constraints. These constraints come in two types: first, single-domain constraints define the set of properties included in the concept, of which exactly one from each included domain must be present; second, cross-domain constraints exclude certain combinations of properties from two or more domains.

Conceptual Space and Concept Definitions

The domain and properties of the collision risk conceptual space described above are mapped to states as follows:

$$\begin{array}{rllll}
\textbf{Propulsion}: & \text{Chemical} = x_{11} & \text{Electrical} = x_{12} & \text{None} = x_{13} & \\
\textbf{Maneuverability}: & \text{Healthy} = x_{21} & \text{Defunct} = x_{22} & & \\
\textbf{Reachability}: & \text{Short} = x_{31} & \text{Medium} = x_{32} & \text{Long} = x_{33} & \text{Never} = x_{34} \\
\textbf{Vulnerability}: & \text{Yes} = x_{41} & \text{No} = x_{42} & &
\end{array}$$

The states are binary in nature with values of either zero (off) or one (on). The Risk concept is defined by the constraints in Table 1.

Table 1. Risk Concept Definition

Domains and Properties	*In Terms of States*
Propulsion $\in$ {Chemical, Electrical}	$x_{11} + x_{12} = 1$
Maneuverability = Healthy	$x_{21} = 1$
Reachability $\in$ {Short, Medium, Long}	$x_{31} + x_{32} + x_{33} = 1$
Vulnerability = Yes	$x_{41} = 1$
$\neg$ (Propulsion = Chemical $\wedge$ Reachability = Medium)	$x_{11} + x_{32} \leq 1$
$\neg$ (Propulsion = Chemical $\wedge$ Reachability = Long)	$x_{11} + x_{33} \leq 1$

The final two constraints are examples of cross-domain constraints. Specifically, these two constraints ensure that Reachability $=$ Medium or Reachability $=$ Long are only considered significantly risky when Propulsion $=$ Electrical. Note that the $\neg$ symbol means "not" and the $\wedge$ symbol means "and". They result in the following set of possible $(\text{Propulsion}, \text{Reachability})$ pairs for a collision risk: $(\text{Chemical}, \text{Short})$, $(\text{Electrical}, \text{Short})$, $(\text{Electrical}, \text{Medium})$, and $(\text{Electrical}, \text{Long})$. The cross-domain constraints are included because spacecraft with electrical (i.e., low-thrust) propulsion typically plan and execute maneuvers over longer timespans than those with chemical (i.e., high-thrust) propulsion. Therefore, the more we believe a spacecraft has electrical propulsion, the more our model views reachability in the medium and long time horizons as a cause for concern.

The corresponding objective function for a given observation $\boldsymbol{s}$ is

$$f_1(\boldsymbol{x} \mid \boldsymbol{s}) = \frac{1}{4} \left(s_{11}x_{11} + s_{12}x_{12} + s_{21}x_{21} + s_{31}x_{31} + s_{32}x_{32} + s_{33}x_{33} + s_{41}x_{41} \right) \tag{2}$$

The Non-Risk concept is defined in Table 2.

Table 2. Non-Risk Concept Definition

Domains and Properties	*In Terms of States*
Reachability $=$ Never	$x_{34} = 1$
Vulnerability $=$ Yes	$x_{41} = 1$

Its corresponding objective function for a given observation $\boldsymbol{s}$ is

$$f_2(\boldsymbol{x} \mid \boldsymbol{s}) = \frac{1}{2} \left(s_{34}x_{34} + s_{41}x_{41} \right) . \tag{3}$$

The Non-Risk concept includes the assumption that Vulnerability $=$ Yes to avoid biasing the result because we assume spacecraft are always vulnerable to collisions. Non-Risk's concept definition could change if other types of on-orbit risk are considered such as communication frequency and resiliency.

Reachability Analysis

This section describes the high- and low-thrust reachability analysis tools. Because this paper is intended as a proof-of-concept for our overall conceptual spaces-based collision risk analysis method, we do not perform actual OD to determine uncertainty in the required Δv for one satellite to reach another. Instead, this uncertainty is simulated in the high-thrust case by defining an arbitrary uniform distribution around the calculated minimum Δv requirement and in the low-thrust case by randomly sampling the initial costates from an arbitrary uniform distribution. In future work, we plan to perform simulated OD and use a Monte Carlo analysis that accounts for the uncertainty estimate it produces.

High Thrust. Quantifying the capability of a chaser satellite to collide with a target in one or two high-thrust maneuvers (or to rendezvous with the target in two or three maneuvers) in this work involves solving Lambert's two-point boundary value problem to generate an initial transfer guess.[10] Starting with initial states for the chaser and target, many Lambert solutions are determined by combining a set of times of flight with a set of wait times (time past the initial state epoch at which the transfer begins). Solutions are ordered by the amount of Δv required (either just for the first burn in cases where collision risk is being judged or the total of the two burns in rendezvous cases). A number of the solutions that require the least amount of Δv are selected as initial guesses for higher fidelity optimization of the chaser to target transfer. The second burn (or middle burn in rendezvous cases) is always initialized as having zero magnitude in all directions.

For each of these initial cases, an optimization process is run. When optimizing for a collision, the cost is equal to the sum of the magnitudes of the first two maneuvers, with the only constraint being that the final position of the two satellites must be the same. When optimizing for rendezvous, the magnitude of the third burn is added to the cost and the final velocities of the two satellites is an added constraint. Solutions are saved after checking to be sure the created trajectory would not cause the chaser to re-enter the atmosphere. The minimum Δv for a solution saved is determined to be the overall minimum cost for the chaser to either impact or rendezvous with the target. The distribution of required Δv is then returned as a uniform distribution over $\pm 7.5\%$ of the calculated minimum value. These steps are repeated for short, medium and long time horizons.

Low Thrust. The low-thrust reachability tool, rather than looking at reachability between a given chaser and target as the high-thrust tool does, generates a space comprised of all reachable states from a given initial chaser state within a specified amount of time. Any potential targets within this space are considered to be reachable for either collision or rendezvous by the chaser. This is accomplished with a large number of propagations from the initial state; each case is given a set of randomly selected costates in the Modified Equinoctial Elements regime. The costate for the semiparameter (p) is randomly selected uniformly between -10 and 10; the costates for all other elements are randomly selected uniformly between -1 and 1. The semiparameter costate is scaled in this way because it was found to encourage significant changes in the size of the orbit in addition to the shape and orientation.

The optimal control over time as a function of the costate vector is defined via Pontryagin's minimum principle, yielding propellant-optimal local solutions to the two-point boundary value problem between the initial state and the final state. The dualized state-costate system for the satellite is propagated for an amount of time randomly selected between zero and the specified reachable time, thus yielding the propellant-optimal reachable set of final states. The satellite is assumed to be thrusting at all times except for when it is in shadow. The final chaser state is collected from each scenario. Orbital elements are collected and plotted. Figure 1 is an example with an initial circular orbit and a semi-major axis of approximately 29,600 km. In addition to eccentricity and semi-major axis, which are featured in Figure 1, inclination and true longitude are useful elements for judging reachable space.

Uncertain Observations

Uncertainty in the initial orbital states of the two space objects and in the maneuvering spacecraft's Δv capacity leads to uncertainty in the reachability domain. This uncertainty is accounted for in the similarity optimization based on the mean and variance of the probability that the maneuvering spacecraft has sufficient Δv available to reach the other spacecraft in each time frame. One spacecraft is reachable by another in a given time frame when the latter's available Δv is greater than the required Δv. If these Δv parameters are assumed to be uniform random variables $a \sim \mathrm{Unif}\,[a_0, a_1]$ (available Δv) and $r \sim \mathrm{Unif}\,[r_0, r_1]$ (required Δv), the probability that the spacecraft is reachable given a particular value of a is

$$\mathrm{P}\{r \le a \mid a\} = \max\left\{0, \min\left\{1, \frac{a - r_0}{r_1 - r_0}\right\}\right\}, \tag{4}$$

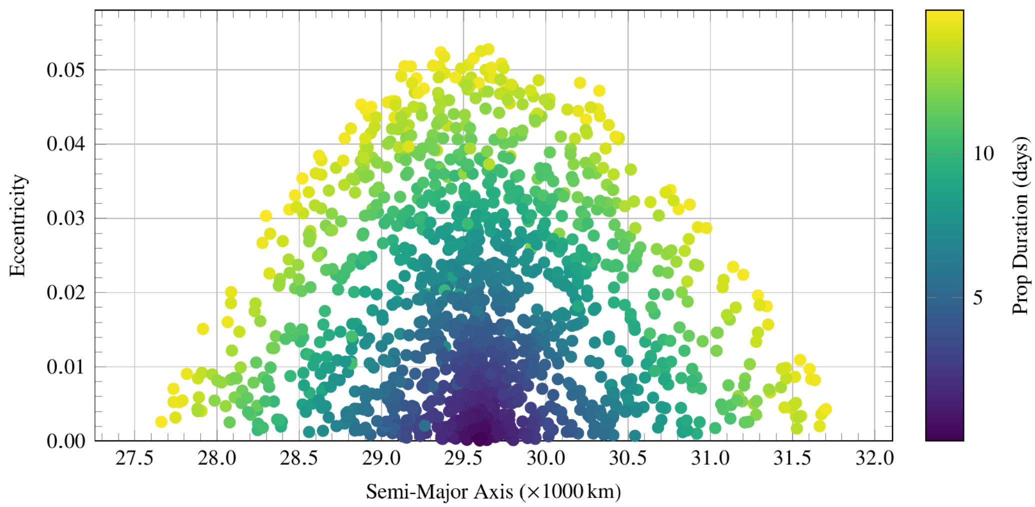

Figure 1. Plot of low-thrust reachable states in 15 days from an example initial chaser satellite state.

and the mean and variance of $\mathrm{P}\{r \leq a\}$ may be found by integrating the relevant expressions over the interval $[a_0, a_1]$.

Bounded Approach (Interpolation). Incorporating uncertain observations into the linear optimization problem in Eq. (1) can be tackled with stochastic linear programming and robust optimization. However, both can be computationally intensive and involve testing numerous scenarios.[11] Below is a novel approach for incorporating the mean and variance of a random variable into the similarity values (the coefficients) of the objective function. It is a way of deriving similarity values using mean and variance that ensures the resulting objective function is properly bounded, with a domain containing properties $A, B, \ldots$ and N ("none of the above"):

$$s_A = \left(1 - \frac{\sigma_A^2}{\sigma_{\max}^2}\right)\mu_A + \frac{\sigma_A^2}{2\sigma_{\max}^2} \tag{5}$$

$$s_B = \left(1 - \frac{\sigma_B^2}{\sigma_{\max}^2}\right)\mu_B + \frac{\sigma_B^2}{2\sigma_{\max}^2} \tag{6}$$

$$\vdots$$

$$s_N = \left(1 - \frac{\max\left\{\sigma_A^2, \sigma_B^2, \ldots\right\}}{\sigma_{\max}^2}\right)(1 - \max\left\{\mu_A, \mu_B, \ldots\right\}) + \frac{\max\left\{\sigma_A^2, \sigma_B^2, \ldots\right\}}{2\sigma_{\max}^2} \tag{7}$$

Note that $\sigma_{\max}^2$ may be derived from the fact that the support of the PDF is restricted to the interval $[0, 1]$. In this work, the most uncertain possible observation is a uniform distribution over that interval, so $\sigma_{\max}^2 = 1/12$.

For example, consider a domain with three properties, with observed means and variances $(0.4, 0.02)$ and $(0.9, 0.01)$ for the first two. Applying the approach described above yields the observed similarity values $s_1 = 0.424$, $s_2 = 0.852$, and $s_3 = 0.196$. If σ_2^2 is increased from 0.01 to 0.06, the results change to $s_1 = 0.424$, $s_2 = 0.612$, and $s_3 = 0.388$. The increased uncertainty in the second property's observation reduces its similarity value and increases that of the "none of the above" third property.

SIMULATION RESULTS

In the presented simulation, we apply our risk conceptual space pointwise in time over the two weeks leading up to the 2009 collision between Iridium 33 and Cosmos 2251.[12] The collision occurred at 16:55:59.82 UTC on February 10, 2009, following a two-burn station-keeping maneuver executed by Iridium 33 earlier that morning. The burns occurred at around 07:11 and 08:01 UTC, respectively, and ultimately drove the satellite to collide with the derelict Cosmos 2251. With the information and techniques available at the time, the operators of Iridium 33 were not aware of the possible collision with Cosmos 2251 until after it had already occurred.

For this simulated analysis, the mixed-integer optimization problem is solved by the COIN-OR branch-and-cut solver with the `PuLP` Python library.[13] Uncertainty in reachability observations is accounted for using the bounded approach described earlier in this paper. Each reachability analysis is performed based on the historical two-line element (TLE) data for the two satellites, as opposed to a full OD simulation. As described in the Reachability Analysis section, we simulate OD uncertainty by computing the minimum Δv required for the spacecraft to collide and then adding bounds of $\pm 7.5\%$ to construct a uniform distribution for the required Δv. Note that this historical example is a high-thrust reachability scenario due to the spacecraft involved. This proof-of-concept demonstration does not make use of the low-thrust reachability tool.

Figure 2 shows the result when the analysis is performed from the perspective of Cosmos 2251, meaning the measurements consumed by the mixed-integer optimization problem describe Iridium 33. This perspective is presented because Iridium 33 can maneuver while Cosmos 2251 cannot, resulting in a more interesting reachability analysis. These results show that our method can flag a potentially risky situation two days before the collision, and more than one day before the maneuver that caused the collision.

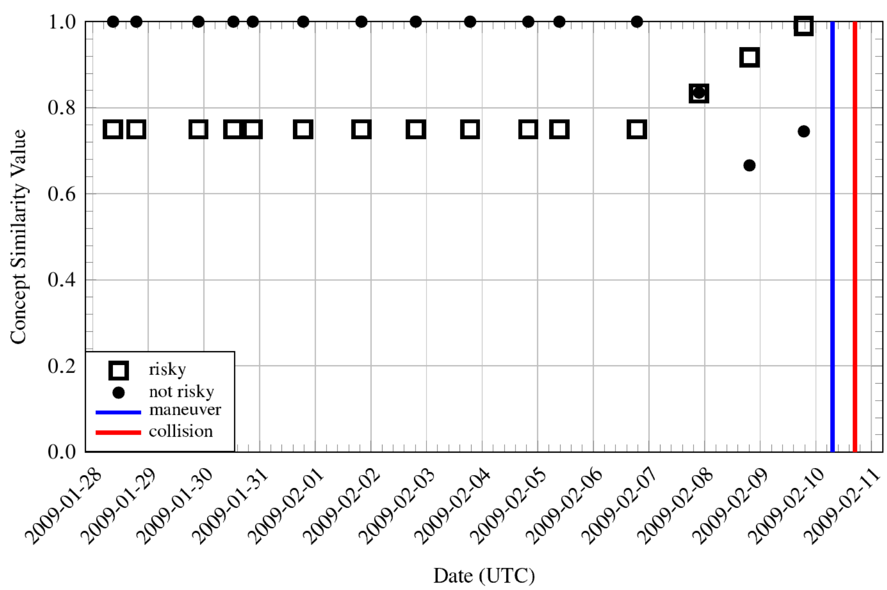

Figure 2. Plot of similarity values for risk and non-risk concepts over the two weeks leading up to the Iridium–Cosmos collision, from the perspective of Cosmos 2251.

Post-mortem analysis of the actual collision shows a range of values for probability of collision depending on the precise scenario and method of calculation. Using data solely from the Joint

Space Operations Center (JSpOC), the 3D probability of collision is $9.5\ \ 10^{-27}$ at 20:00 UTC on February 8, $2.6\ \ 10^{-51}$ at 20:00 UTC on February 9, and $4.9\ \ 10^{-4}$ approximately one hour before the collision on February 10.[12] Therefore, with a threshold of 10^{-4}, the JSpOC analysis would only flag the possible collision after the maneuver. On the other hand, a collision probability analysis using Iridium's private OD solution produces values of $7.5\ \ 10^{-11}$, $1\ \ 10^{-3}$, and $7.4\ \ 10^{-2}$, respectively, which could have flagged the possible collision risk late on February 9.[12] Crucially, however, Iridium's OD data was not available to the JSpOC at the time, causing them to underestimate the pre-maneuver collision probability. Using only publicly available data from the time (i.e., historical TLEs), our model provides an earlier justification for action.

Figures 3 and 4 show the results for the same scenario but with modified definitions of the objective function. Specifically, the terms $s_{ij}x_{ij}$ in the objective function have been assigned arbitrary weights based on their respective domain i. In Figure 3, the Propulsion and Maneuverability domains have half the weight of the other domains, reflecting the fact that both domains together describe satellite's maneuvering capability. This has a small effect on the results in this case, primarily in decreasing ambiguity in the third-to-last set of observations. In Figure 4, Reachability has ten times the weight of the other domains. This significantly changes the numerical values of the concept similarity results but again has the primary effect of resolving the ambiguity in processing the third-to-last set of observations. Though neither weighting has a significant effect on when the risky situation is detected, these two plots demonstrate that domain weights may be adjusted to tune the analysis's sensitivity to different types of observations.

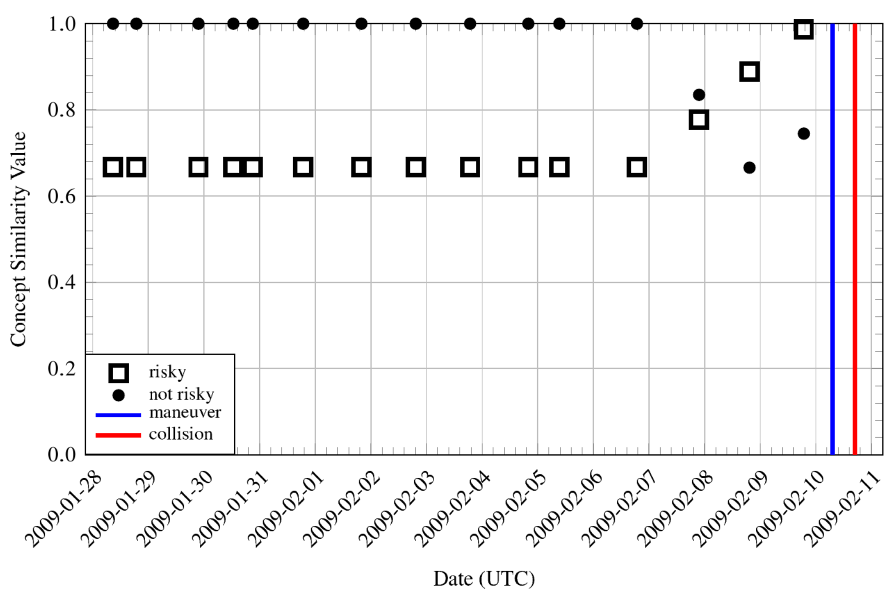

Figure 3. Plot of similarity values for risk and non-risk concepts with equalized domain weights.

Finally, Figure 5 shows results for the same scenario but with the observed value for Iridium 33's Maneuverability $=$ Healthy property reduced from 1 to 0.5. This setup demonstrates how soft information affects our collision risk analysis: As demonstrated by the previous figure, observed short-term reachability in this scenario grows over the final four days before the collision, reaching a value close to 1. However, because the risk concept definition requires that the chaser can maneuver, reducing its observed maneuverability makes the result less sensitive to observed reachability. In this

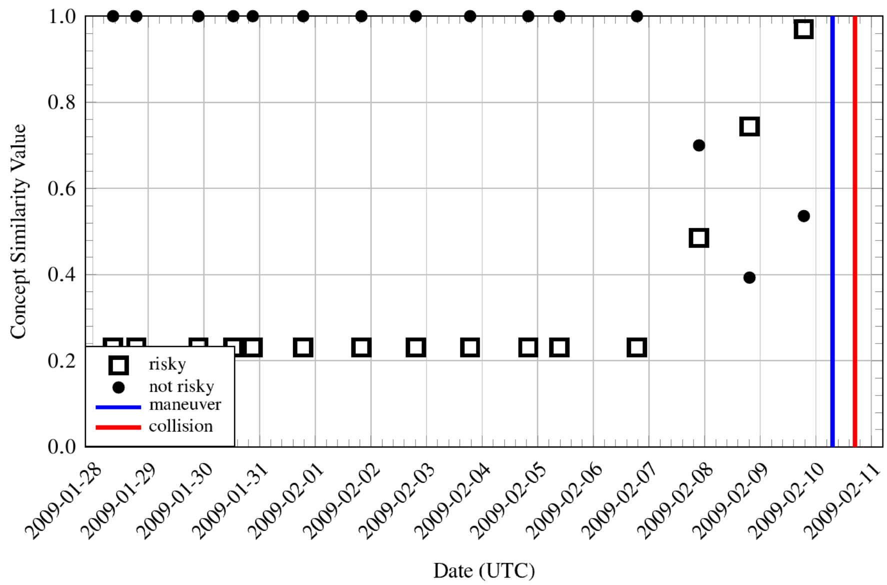

Figure 4. Plot of similarity values for risk and non-risk concepts with increased weight on the reachability domain.

case, where the collision is almost entirely due to the chaser's ability to maneuver, this is a desirable result. However, our conceptual space definition will need to be adjusted to manage situations in which orbit uncertainty plays a more significant role because two defunct spacecraft may still pose a collision risk to one another.

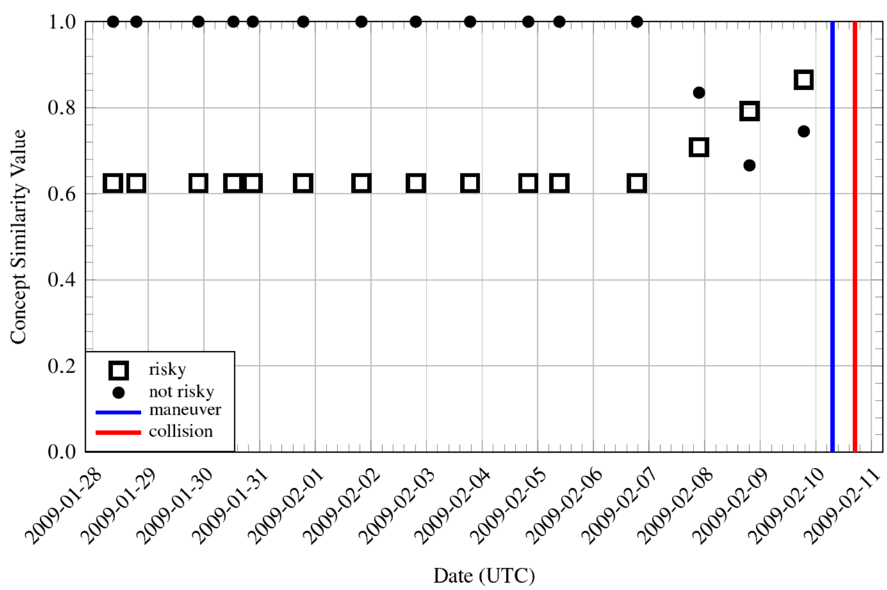

Figure 5. Plot of similarity values for risk and non-risk concepts with 50% confidence in maneuverability.

CONCLUSION AND FUTURE WORK

Conceptual spaces offer a unique method for hard and soft information fusion that can be used for collision risk assessment. We have shown that our model can identify collision risk earlier than a standard probability of collision analysis. Furthermore, it can be tuned for a particular operator's use case through selective weighting in the objective function. This conceptual space setup incorporates uncertainty from the observations related to reachability to bring it closer to reality.

The methodology presented in this paper could be used in tandem with traditional probability of collision analysis to create a more robust system for SSA and collision avoidance. Probability of collision would remain the primary technique for flagging imminent collision risks, but the proposed model could identify pairs of satellites that warrant additional consideration. Such an outcome could justify tasking sensors to collect more frequent observations to monitor changes in their probability of collision or informing satellite owners to proceed with increased caution when planning maneuvers.

Future work may include refining concept definitions, Monte Carlo analysis for more accurate characterization of the reachability uncertainty, stressing the model against both low and high thrust scenarios, and exploring the overall risk of collision in scenarios involving more than two space objects. Incorporating uncertainty directly into the soft information may be feasible through chance constraints. Assessing this method's false negative and false positive rates when applied to simulated and historical scenarios, such as Iridium–Cosmos, will be important for refining it and further comparing its usefulness to traditional collision probability calculations.

ACKNOWLEDGMENT

This material is based on research sponsored by the Air Force Research Laboratory (AFRL) under agreement number FA8750-23-C-1013. The views and conclusions contained herein are those of the authors and should not be interpreted as necessarily representing the official policies or endorsements, either expressed or implied, of the Air Force Research Laboratory.

REFERENCES

[1] U. S. G. A. Office, "Defense Acquisitions Annual Assessment: Drive to Deliver Capabilities Faster Increases Importance of Program Knowledge and Consistent Data for Oversight," Report GAO-22-105166, Government Accountability Office, Washington, D.C., Apr. 2022.

[2] N. Sánchez-Ortiz, M. Belló-Mora, and H. Klinkrad, "Collision avoidance manoeuvres during spacecraft mission lifetime: Risk reduction and required δV," *Advances in Space Research*, Vol. 38, No. 9, 2006, pp. 2107–2116, https://doi.org/10.1016/j.asr.2005.07.054.

[3] E. M. Polli, J. L. Gonzalo, and C. Colombo, "Analytical model for collision probability assessments with large satellite constellations," *Advances in Space Research*, Vol. 72, No. 7, 2023, pp. 2515–2534, https://doi.org/10.1016/j.asr.2022.07.055.

[4] M. Holender, R. Nagi, M. Sudit, and J. T. Rickard, "Information fusion using conceptual spaces: Mathematical programming models and methods," *Proceedings of the 10th International Conference on Information Fusion*, July 2007.

[5] J. T. Rickard, "A concept geometry for conceptual spaces," *Fuzzy Optimization and Decision Making*, Vol. 5, Oct. 2006.

[6] L. Bechberger and K.-U. Kühnberger, "Towards grounding conceptual spaces in neural representations," *Proceedings of the 12th International Workshop on Neural-Symbolic Learning and Reasoning*, July 2017.

[7] J. R. Chapman, D. Kasmier, D. Limbaugh, S. R. Gagnon, J. L. Crassidis, J. Llinas, B. Smith, and A. P. Cox, "Conceptual space modeling for space event characterization," *Proceedings of the 23rd International Conference on Information Fusion*, July 2020.

[8] J. R. Chapman, D. Kasmier, D. Limbaugh, S. R. Gagnon, J. L. Crassidis, J. Llinas, B. Smith, and A. P. Cox, "Utilizing complex conceptual spaces modeling for space situational awareness," *Proceedings of the 2021 AIAA SciTech Forum*, Jan. 2021.

[9] J. R. Chapman, J. L. Crassidis, J. Llinas, B. Smith, D. Kasmier, and A. P. Cox, "Space situational awareness using Dempster-Shafer theory in conceptual spaces modeling," *Proceedings of the 2022 AIAA SciTech Forum*, Jan. 2022.

[10] D. Izzo, "Revisiting Lambert's problem," *Celestial Mechanics and Dynamical Astronomy*, Vol. 121, Oct. 2014, pp. 1–15.

[11] J. J. Torres, C. Li, R. M. Apap, and I. E. Grossmann, "A Review on the Performance of Linear and Mixed Integer Two-Stage Stochastic Programming Software," *Algorithms*, Vol. 15, No. 4, 2022, 10.3390/a15040103.

[12] R. Shepperd, "Subsequent analysis of the collision between Iridium 33 and COSMOS 2251," *Proceedings of the 2023 Advanced Maui Optical and Space Surveillance Technologies Conference*, Sept. 2023.

[13] J. Forrest *et al.*, "COIN-OR/Cbc release 2.10.11," Oct. 2023. `https://github.com/coin-or/Cbc`.